UCRL-JRNL-223961

Measurement of the relaxation time of hot electrons in laser-solid interaction at relativistic laser intensities

H. Chen, R. Shepherd, H. K. Chung, G. Dyer, A. Faenov, K. B. Fournier, S. B. Hansen, J. Hunter, A. Kemp, T. Pikuz, Y. Ping, K. Widmann, S. C. Wilks, P. Beiersdorfer

August 24, 2006

Physical Review E

Measurement of the relaxation time of hot electrons in laser-solid interaction at relativistic laser intensities

H. Chen[1], R. Shepherd[1], H. K. Chung[1], G. Dyer[2], A. Faenov[3], K. B. Fournier[1], S. B. Hansen[1], J. Hunter[1], A. Kemp [4], T. Pikuz[3], Y. Ping[1], K. Widmann[1], S. C. Wilks[1], and P. Beiersdorfer[1]

[1]*Physics and Advanced Technologies, Lawrence Livermore National Laboratory, University of California, Livermore, CA 94550*

[2]*Department of Physics, University of Texas, Austin, Texas*

[3]*Multicharged Ion Spectra Data Center, VNIIFTRI, Mendeleevo, Moscow oblast, 141570 Russia and*

[4] *Department of Physics, University of Nevada, Reno*

(Dated: August 24, 2006)

Abstract

We have measured the relaxation time of hot electrons in short pulse laser-solid interactions using a picosecond time-resolved x-ray spectrometer and a time-integrated electron spectrometer. Employing laser intensities of 10^{17}, 10^{18}, and 10^{19} W/cm^2, we find increased laser coupling to hot electrons as the laser intensity becomes relativistic and thermalization of hot electrons at timescales on the order of 10 ps at all laser intensities. We propose a simple model based on collisional coupling and plasma expansion to describe the rapid relaxation of hot electrons. The agreement between the resulting K_α time-history from this model with the experiments is best at highest laser intensity and less satisfactory at the two lower laser intensities.

It is well established that high-intensity lasers incident on solid targets can generate relativistic electrons [1, 2] through interactions with the laser electric field or the associated ponderomotive force. These hot electrons can effectively heat the solid target beyond the region of direct laser interaction. This is an important aspect of the fast ignition concept, part of a major effort to generate controlled thermonuclear fusion [3]. How hot electrons couple to the bulk solid target is an important open question, since many applications rely on assumed rapid coupling of hot electrons to background thermal electrons. In fast ignition, for example, the coupling must be faster than the time for the compressed core to hydrodynamically disassemble, which is currently thought to be less than about 20 ps [3].

K_α inner-shell radiation, generated when hot electrons excite the core electrons of atoms in the solid, provides a diagnostic for the presence of hot electrons. In fact, measurements of absolute K_α radiation intensity are commonly used to estimate the number of hot electrons generated during the complex laser-target interaction [4–8]. Although, the time-history of K_α emission has been previously measured [9–12] for a laser intensity lower than 10^{17} W/cm^2, up to now, K_α measurements at relativistic laser intensities have all been time-integrated and have thus given no insight into the time scale of the hot electron coupling. A direct, time-resolved measurement of the K_α signal gives a direct determination of this coupling time, significantly increasing our understanding of the physical process of hot electron relaxation. This paper presents the first time-resolved observation of the relaxation of hot electrons generated by a short-pulse, high-intensity laser.

The experiment was performed at the Compact Multipulse Terawatt (COMET) laser facility [13] at Lawrence Livermore National Laboratory. COMET is a hybrid chirped pulse amplification (CPA) system with a Ti:sapphire oscillator and regenerative amplifier with a four-stage Nd:phosphate glass amplifier. The laser wavelength is 1054 nm. For the data presented in this paper, the laser pulse was $p-$polarized with a length of 500 fs at full width at half maximum (FWHM). The laser energy (6–7 J) was focused with an $f/3.6$ parabola onto a solid target at an incident angle of 45.° The best focus was typically 8-10 μm FWHM, resulting in a laser intensity of 10^{19} W/cm^2 at the best focus. By systematically increasing the spot size on the target, we were able to decrease the laser intensity down to 10^{17} W/cm^2 while keeping the laser energy constant.

Pre-pulse is a major concern in short-pulse, laser-solid experiments. The temporal intensity contrast of the pulses is characterized by three components: 1) a 12 ns pre-pulse produced by leakage in the regenerative amplifier, 2) amplified spontaneous emission (ASE), and 3) a pedestal produced by the third and fourth order aberrations in the stretcher. Often, the most significant pre-pulse comes from the leakage pulse from the regenerative amplifier. Using two Pockels cells and polarizers, a contrast of $I_{leakage}/I_{main} \approx 10^{-9}$ was obtained. No measurement was made of the contribution of ASE or third and fourth order aberrations. However, an analysis of the spectrum from the stretcher-compressor system suggest the contribution of the third and fourth order aberrations to non-Gaussian components produce a contrast of $I_{aberr}/I_{main} \approx 10^{-5}$ at about 2 ps before the peak of the pulse [14]. To confirm that the ASE level produced no pre-formed plasma, solid targets were illuminated without seeding the amplifiers with the oscillator pulse. No damage was observed, suggesting minimal effect from ASE. As a monitor of the pre-formed plasma, a visible spectrometer was set up to look at the specular reflected laser light. Because Raman scattering and two-plasmon decay are a strong function of density scale length [15], the spectrally resolved, specular light provided a shot-to-shot monitor of large fluctuations in the pre-pulse. We observed mostly constant harmonic spectra throughout the experiments, indicating stable preplasma conditions during the laser-target interactions.

The laser targets consisted of $12.5 \mu m$ of Ti over-coated with 1000 Å of Al. The Al layer prevented direct illumination of the Ti foil, thus eliminating any direct laser heating. The x-ray emission from the target was collected using the Time REsolved X-ray Streak (TREX) camera [16] interfaced to two crystals arranged in the von Hàmos geometry: a graphite crystal withan 11 cm radius of curvature (R_c) to collect the Ti K$_\alpha$ emission and a second crystal with $R_c = 3$ cm to collect the Al K-shell 1s2p(^{1}P)-1s^2(^{1}S) (He$_\alpha$) emission. The streak camera was coupled to an image intensifier, a 2:1 fiber optic reducer, and a fiber optic face plate mounted on a 16-bit, water-cooled, 1024 x 1024 pixel CCD. The time resolution of the streak camera is about 1ps, and the total coverage is about 40 ps. A time-integrated measurement of the electrons escaping the target was made using an absolutely calibrated Fiber-optic Array Compact Electron Spectrometer (FACES) [17], which was set up to measure electrons from 80 keV to 6 MeV. It was positioned 37 cm behind the target, 15° off the laser propagation direction with a solid angle of 1×10^{-4} steradians. Finally, a time-integrated, spatially resolved x-ray spectrometer with a spherically bent quartz crystal was fielded to view the back surface of the target, providing high-resolution spectra from which the heating of the Ti target was determined [18].

Data were collected at laser focal intensities of 10^{17}, 10^{18}, and 10^{19} W/cm^2, spanning the transition from non-relativistic ($P_{os}/(m_e c)$=0.3) to relativistic ($P_{os}/(m_e c)$=3) laser intensities, where P_{os} is the electron momentum and m_e the electron mass. Figure 1 shows that significantly more hot electrons were observed by the electron spectrometer as the laser intensity became relativistic: the number of $\approx$ 100 keV electrons per keV increases from 4×10^5 for $I = 10^{17}$, to 9×10^5 for $I = 10^{18}$, and to 2×10^6 for $I = 10^{19}$ W/cm^2. This increase is consistent with the measured enhanced laser absorption at higher laser intensities described in Ref. [19]. A quantitative description of the hot electron energy distribution is the so-called "hot electron temperature" T_h, obtained by fitting the spectrum with one or more quasi-Maxellian distribution functions. To estimate T_h right after the laser pulse from the time integrated spectra, we fit a Maxwellian to the high end of the energy distribution, reasoning that the hot electron energy can only decrease after the laser pulse is turned off. Fits to the high end of the electron distribution give T_h = 100, 270, and 520 keV for laser intensities of 10^{17}, 10^{18}, and 10^{19} W/cm^2, respectively. These temperatures agree approximately with the ponderomotive scaling of hot electrons [20] except for the highest intensity, where the measured T_h is about half of the predicted value.

The angular dependence of the hot electron distributions from short-pulse solid interactions has been determined experimentally and explained theoretically [19, 21–27]. For our case (a high contrast p-polarized laser incident at 45° to a foil target), the most dramatic angular variations would be due to collimated hot electron jets. At intensities of 10^{17} and 10^{18} W/cm^2, these jets form mostly in the specular and target normal directions at the front of the target [22, 27, 28] and are driven by resonant absorption. At 10^{19} W/cm^2, another jet forms at the back of the target due to poderomotive heating. The angle of this jet is predicted to be about 20° off the laser direction [26, 27]. Since the FACES measurement looks at the back of the target 15° off the laser direction, it is not in the path of the possible jets and may underestimate both the total number of electrons and their maximum energies.

Although the large majority of hot electrons at the measured T_h pass unperturbed through the thin Al layer on the front of the target, the 1000 Å Al is heated by both direct interactions with the incident laser and by the laser-generated hot electrons. Measurements of Al K-shell emission from the TREX spectrometer at wavelengths between 7.6 and 7.9 Å indicate significant heating but little expansion of the Al layer: We observed a prominent Al He$_\alpha$ line at 7.765 Å, but detected neither a strong intercombination line ($1s^2(^1S)$ – $1s2p(^3P)$)

at 7.806 Å nor significant satellite emission from Li-like or lower-charged Al ions. The absence of the density-sensitive intercombination line (whose upper level is a metastable state that is collisionally depopulated at densities higher than 10^{21} cm^{-3} [29]) indicates that no significant pre-plasma is formed before the arrival of the main pulse, confirming the prepulse and Raman measurements discussed above.

Shielded by the Al layer from direct laser heating, the Ti layer mostly interacts with hot electrons that excite and ionize K-shell electrons and produce Ti K_α emission. Because the decay of the upper ($n = 2$) level is extremely rapid, occurring in about 5 fs for Ti $K_{\alpha 1}$ [30], the Ti K_α intensity is limited by the rate of electron-impact ionization of the $n = 1$ level. The intensity is thus $I_{K_\alpha} \propto \int_{V,E} n_i n_e(E)\sigma(E) v_e dV dE$, where n_i is the solid density of Ti, $n_e(E)$ the electron density at energy E, $\sigma(E)$ the cross section of electron impact ionization at energy E, and v_e the velocity of electrons. The integral is over the emission volume V and electron energy E. Figure 2 shows the time history of the measured Ti K_α intensities for the three laser intensities. We measure the hot-electron relaxation time (defined as the FWHM of I_{K_α}) to be 15.9, 13.2, and 12.3 ps, for laser intensities of $10^{19}, 10^{18}$, and 10^{17} W/cm^2, respectively.

Note that the K_α emission durations in our experiment are significantly larger than those measured previously [9–12]. This is due to the fact that (i) our hot electron temperatures are at least one order of magnitude larger; (ii) as a consequence, the hot electron range here is many times the target thickness so that multiple interaction and K_α generation can occur with parts of the target that are transparent for $K\alpha$ radiation. This is not the case in the earlier measurements quoted; (iii) we use different materials with a larger threshold energy for K_α.

Collisions between the hot electrons and the bulk thermal electrons increase the temperature of the bulk target. An analysis of spherical crystal spectrometer measurements indicated a final bulk temperature $T_c \approx 50$ eV and an average Ti ion charge of 4 – 5 [18]. The Al layer is also heated partially by the hot electrons and remains hot enough to emit significant Al He_α radiation long after the Ti K_α emission has decayed. The inset of Fig. 2 shows the Al He_α emission over at least 40 ps (the time coverage of the streak camera). We have not been able to quantify how much of the Al plasma heating is due to the hot-electron relaxation and how much is due to direct interactions with the laser.

We have developed an expanding multi-component plasma model to help understand the measured hot-electron relaxation times. In this model, the hot electrons can lose energy in two ways: through adiabatic cooling due to plasma expansion and through direct collisions which transfer energy from the hot electrons to cold electrons and ions.

The expansion of the plasma is determined mostly by the ion sound speed [31]. Since the hot electrons move much faster than the ions ($v_i < 0.1\,c$ for protons typically), T_h evolves adiabatically according to $p \propto V^\gamma$, where the volume V is defined by the ion-front position. Combining expansion and collisions gives:

$$\frac{dT_h}{d\,t} = \nu_\epsilon^{hc}\,(T_c - T_h), + \alpha\, V(t)^{-\gamma}\, dV(t)/d\,t \tag{1}$$

$$\frac{dT_c}{d\,t} = \nu_\epsilon^{ch}\,(T_h - T_c)\ , \tag{2}$$

where ν_ϵ^{hc} is an energy transfer rate between hot and cold electrons given by

$$\nu_\epsilon^{hc} = \frac{8\,\sqrt{2\,\pi}\,e^4}{3}\,\frac{Z_h^2\,Z_c^2\,n_c\,\ln\Lambda}{(m_e\,(kT_c + kT_h))^{3/2}} \tag{3}$$

Here, $\alpha = T_{h,0}\,V_0^{\gamma-1}$ depends on the initial hot electron temperature $T_{h,0}$ and the initial target volume V_0, and $\gamma = 5/3$. The above equations have to be complemented by an adequate model for the ion-front position [31], details of which will be described elsewhere [32]. Figure 3 shows the predictions of this simplified relaxation model under conditions that are roughly comparable to the experiment for a laser intensity of 10^{19} W/cm^2 (Fig. 3 (a)) along with the dependence of the relaxation time on the initial hot electron temperature (Fig. 3 (b)). The model predicts an initial drop in T_h over the first ≈ 5 ps due to expansion and a equilibration after ≈ 20 ps due to collisions. The final bulk temperature of a few tens of eV is in good agreement with [18].

Applying the measured hot electron temperature and its relaxation profile from the above model to the time-dependent collisional-radiative FLYCHK [33] code, we derive the Ti K_α emissivity as a function of time, assuming that K_α radiation is related only to the laser-generated hot electron population. As shown in Fig. 4 for the case of 10^{19} W/cm^2, the time duration (10–20 ps) of the modelled K_α is close to that measured by the experiment (15.9 ps). For the two lower laser intensities, the agreement between modeled K_α duration (2–10 ps) and the measurements (12 –13 ps) is less satisfactory. Moreover, even when the model matches the decay of the K_α intensities, it does not reproduce the measured rise. Since we do not have a timing fiducial, we do not know when the main laser pulse occurred relative to the K_α signal. Unlike earlier studies at lower laser intensities (10^{14}–10^{17} W/cm^2) [10–12] where the measured K_α burst time was close to the laser duration, the main pulse (500 fs) and K_α signal (10–15 ps) cannot be coincident in our experiment.

Assuming that the main laser pulse occurs before the maximum K_α intensity, there are two possibilities for the few-ps measured rise in K_α. The first is that the early K_α signal is due to hot electrons generated well before the peak of the laser pulse. In this scenario, the K_α emission rises along with the laser intensity, reaching its maximum near the time of peak laser intensity. While we do not expect the prepulse to produce measurable K_α given the measured laser contrast, a non-Gaussian component due to imperfection in the recompression could contribute to the population of K_α generating electrons before the peak in the laser pulse. The second, more plausible, possibility is that the main pulse occurs well before the K_α intensity peak, creating an initial population of hot electrons that both directly generates K_α photons via inner-shell processes and creates secondary "K_α electrons" via ionization of valence shell electrons (i.e., electrons with sufficient energy to produce further inner-shell ionizations). Since the rate coefficient for valence-shell ionization is several hundred times that of inner-shell ionization, only a small fraction of these secondary electrons need to have sufficient energy to produce K_α emission in order to overwhelm the direct K_α production by the primary hot electrons. In this scenario, the risetime (and indeed the majority of the K_α production) is attributable to these secondary K_α electrons. Future measurements may be able to resolve the origin of the K_α rise with timing fiducials.

In conclusion, we have measured the relaxation time of hot electrons produced in short-pulse laser-solid interactions at relativistic laser intensities. We find increased laser coupling to hot electrons as the laser intensity becomes relativistic and a much longer (on the order of 10 ps) duration of K_α emission than the temporal duration of the main laser pulse. The time-scale observed (12 - 16 ps) is still short enough to allow laser-driven hot electrons to be useful for fast-ignitor energy deposition. We have proposed a simple model based on collisional coupling and plasma expansion. The agreement between the resulting K_α time-history from this model with the experiments is best at highest laser intensity and less satisfactory at the two lower laser intensities. We also discussed the possible effect on the time history of K_α from the secondary "K_α electron" generation from the interaction between the primary hot electrons and the target.

This work was performed under the auspices of the U.S. Department of Energy by University of California Lawrence Livermore National Laboratory under contract No. W-7405-

Eng-48.

---

[1] M. H. Key, et al., Phys. Plasmas **5**, 1966 (1998)

[2] S. P. Hatchett, et al., Phys. Plasmas **7**, 2076 (2000)

[3] M. Tabak, et al., Phys. Plasmas **1**, 1626 (1994)

[4] K. B. Wharton, et al., Phys. Rev. Lett. **81**, 822 (1998)

[5] R. A. Snavely, et al., Phys. Rev. Lett. **85**, 2945 (2000)

[6] F. Pisani, et al., Phys. Rev. E **62**, R5927 (2000)

[7] Ch. Reich, et al., Phys. Rev. E **68**, 056408 (2003)

[8] D. Riley, et al., Phys. Rev. E **71**, 016406 (2005)

[9] U. Andiel, K. Eidmann, K. Witte, I. Uschmann and E. Förster, Appl. Phys. Lett. **80**, 198 (2002)

[10] Ch. Reich, P. Gibbon, I. Uschmann and E. Förster, Phys. Rev. Lett. **84**, 4846 (2000)

[11] E. Pisani, U. Andiel, K. Eidmann, K. Witte, I. Uschmann, A. Morak, E. Fö rster and R. Sauerbrey, Appl. Phys. Lett. **84**, 2772 (2004)

[12] T. Feurer, A. Morak, I. Uschmann, Ch. Ziener, H. Schwoerer. Ch. Reich, P. Gibbon, E. Förster and R. Sauerbrey, Phys. Rev. E **65**, 016412 (2001)

[13] J. Dunn, et al., Opt. Lett. **24**, 101 - 103 (1999)

[14] J. Dunn, et al., in AIP Conf. Proc. vol. **369** "Laser Interaction and Related Plasma Phenomena", ed. S. Nakai and G.H. Miley, pp. 652 - 659 (American Institute of Physics Press: Woodbury, New York, 1996)

[15] Liu, C. S. and M. N. Rosenbluth, Phys. Fluids **19**, 967 (1976); L. Veisz, W. Theobald, T. Feurer, H. Schwoerer, I. Uschmann, O. Renner, and R. Sauerbrey, Phys. Plasma. **11**, 3311 (2004)

[16] R. Shepherd, et al., Rev. Sci. Instrum. **75**, 3765 (2004)

[17] H. Chen, et al., Rev. Sci. Instrum. **74**, 1551, (2003)

[18] S. B. Hansen; et al., Phys. Rev. E **72**, 036408, (2005)

[19] Y. Ping, et al., submitted (2006)

[20] S. C. Wilks, W. L. Kruer, M. Tabak, and A. B. Langdon, Phys. Rev. Lett. **69**, 1383 (1992)

[21] G. Malka and J. L. Miquel, Phys. Rev. Lett. **77**, 75 (1996)

[22] D. F. Cai, et al., Phys. Plasmas **10**, 3265 (2003)

[23] Y. T. Li, et al., Phys. Rev. Lett. **96**, 165003 (2006)

[24] S. Bastiani, et al., Phys. Rev. E **56**, 7179, (1997)

[25] Y. T. Li, et al., Phys. Rev. E **69**, 036405, (2004)

[26] H. Rühl, et al., Phys. Rev. Lett. **82**, 743 (1999)

[27] Y. Sentoku, et al., Phys. Plasmas **6**, 2855 (1999)

[28] D. F. Cai, et al., Phys. Rev. E **70**, 066410, (2004)

[29] D. Duston, et al., Phys. Rev. A **28**, 2968, (1983)

[30] J. Scofield, Phys. Rev. A **9**, 1041, (1974)

[31] P. Mora Phys. Rev. Lett. **90**,185002 (2003)

[32] A. Kemp, et al., to be published, (2006)

[33] H-K.,Chung, et al, High Energy Density Physics **1**, 3, (2005)

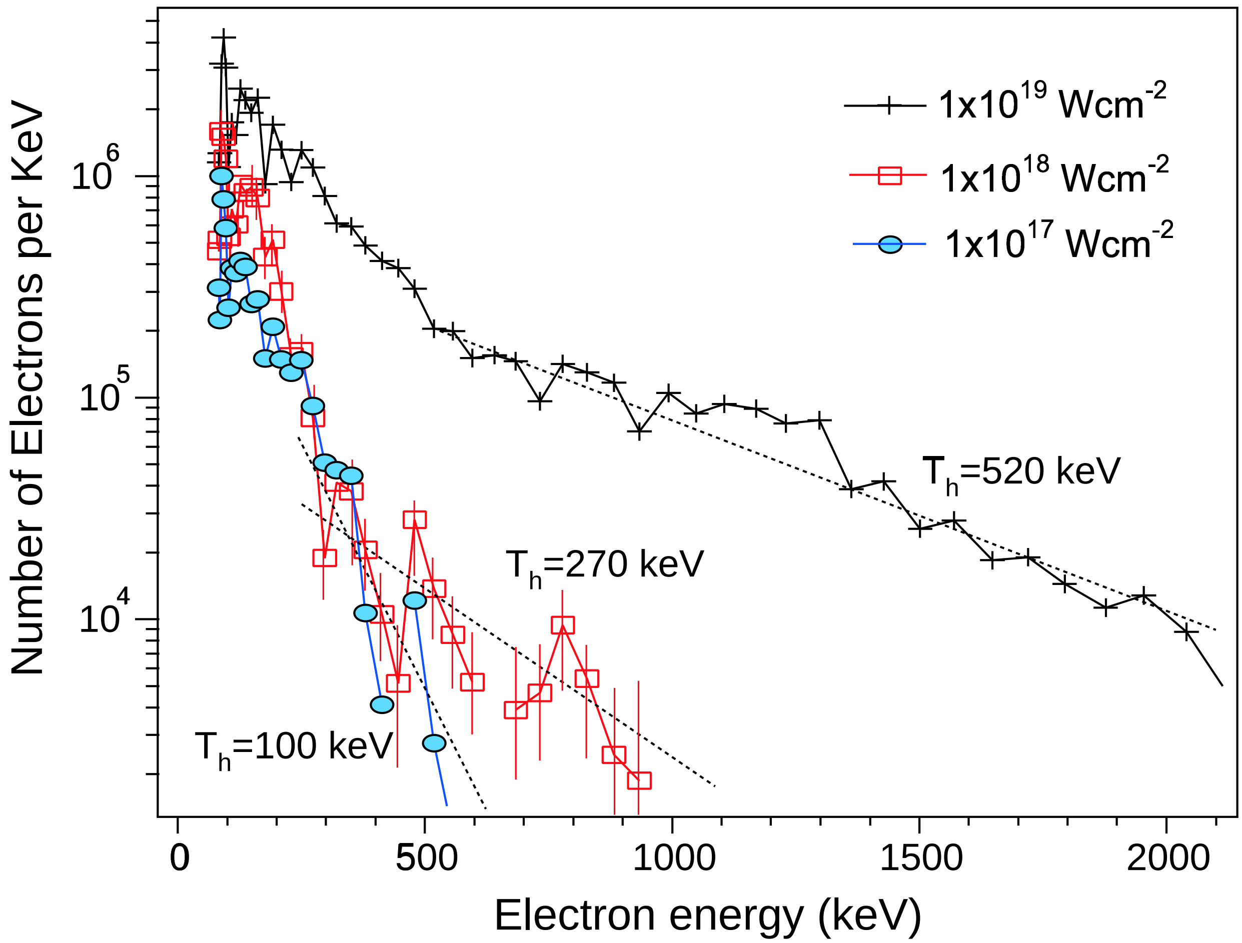

FIG. 1: Electron spectroscopy data from FACES for the three laser intensities. Error bars of the measurement are marked for the medium intensity. The dotted lines are the exponential fit to the high energy section of the spectra.

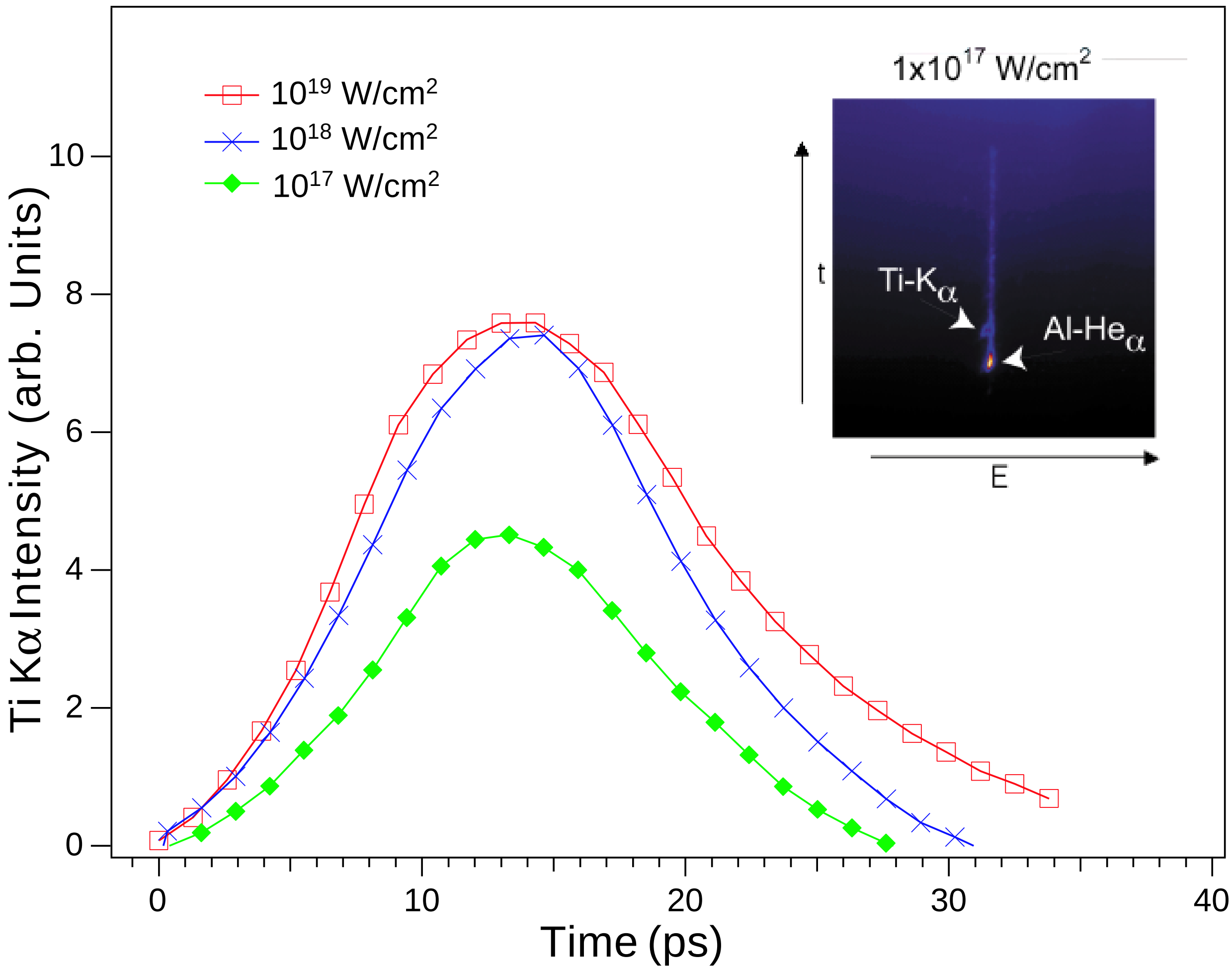

FIG. 2: Ti K_α line intensity as a function of time at the three laser intensities. The full width at half maximum is 15.9 ps, 13.2 ps and 12.3 ps measured at laser intensities of 1×10^{19}, 1×10^{18}, and 1×10^{17} W/cm^2, respectively. The inset is a streak image from TREX at laser intensity of 10^{17} W/cm^2.

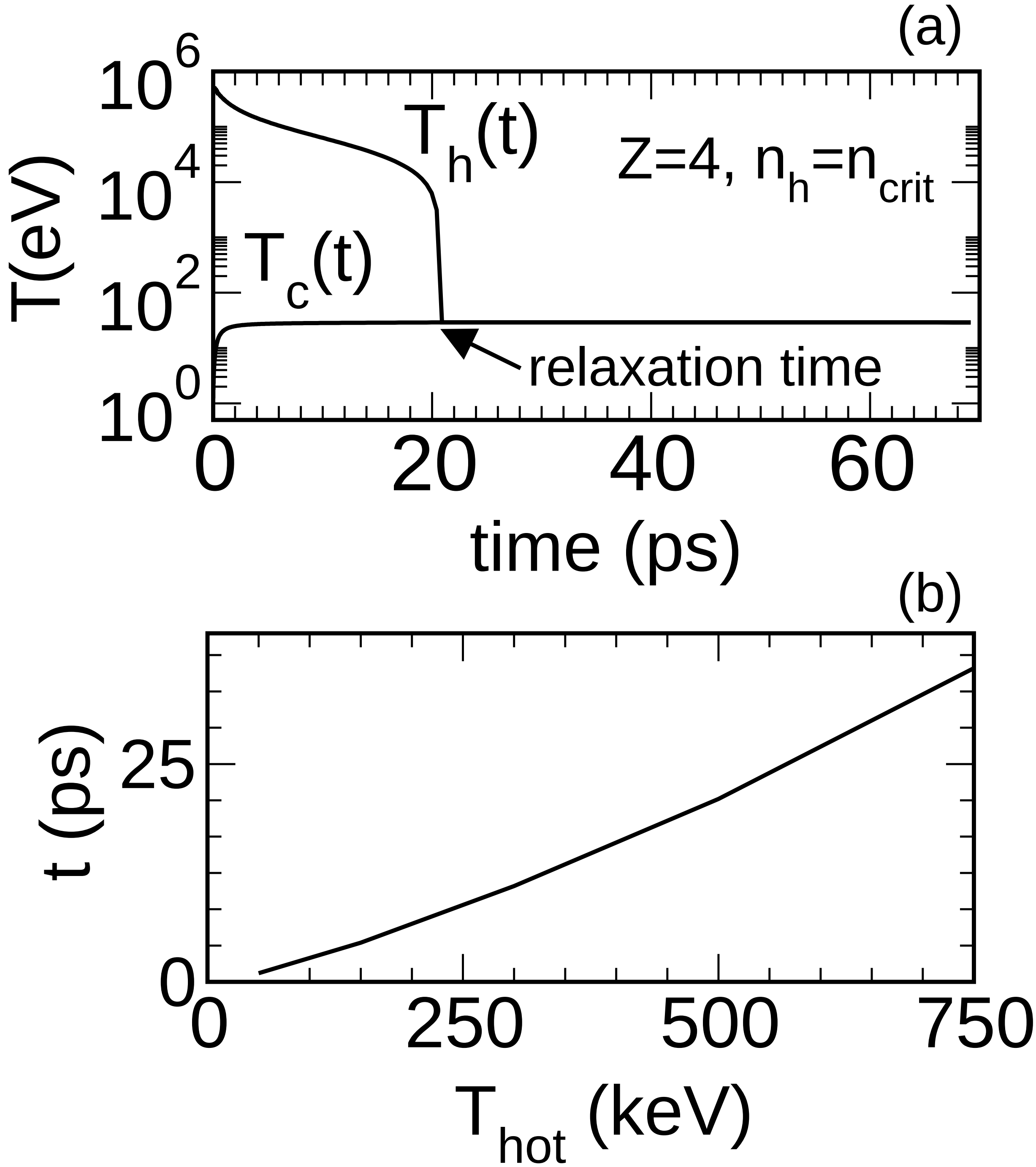

FIG. 3: Predicted relaxation time of hot and cold electrons in a solid density Ti^{+4} plasma with $n_{\rm hot} = 10^{21}\,{\rm cm}^{-3}$ according to our simple model. (a) Evolution of hot and cold electron temperatures. (b) Relaxation time vs. initial hot electron temperature.

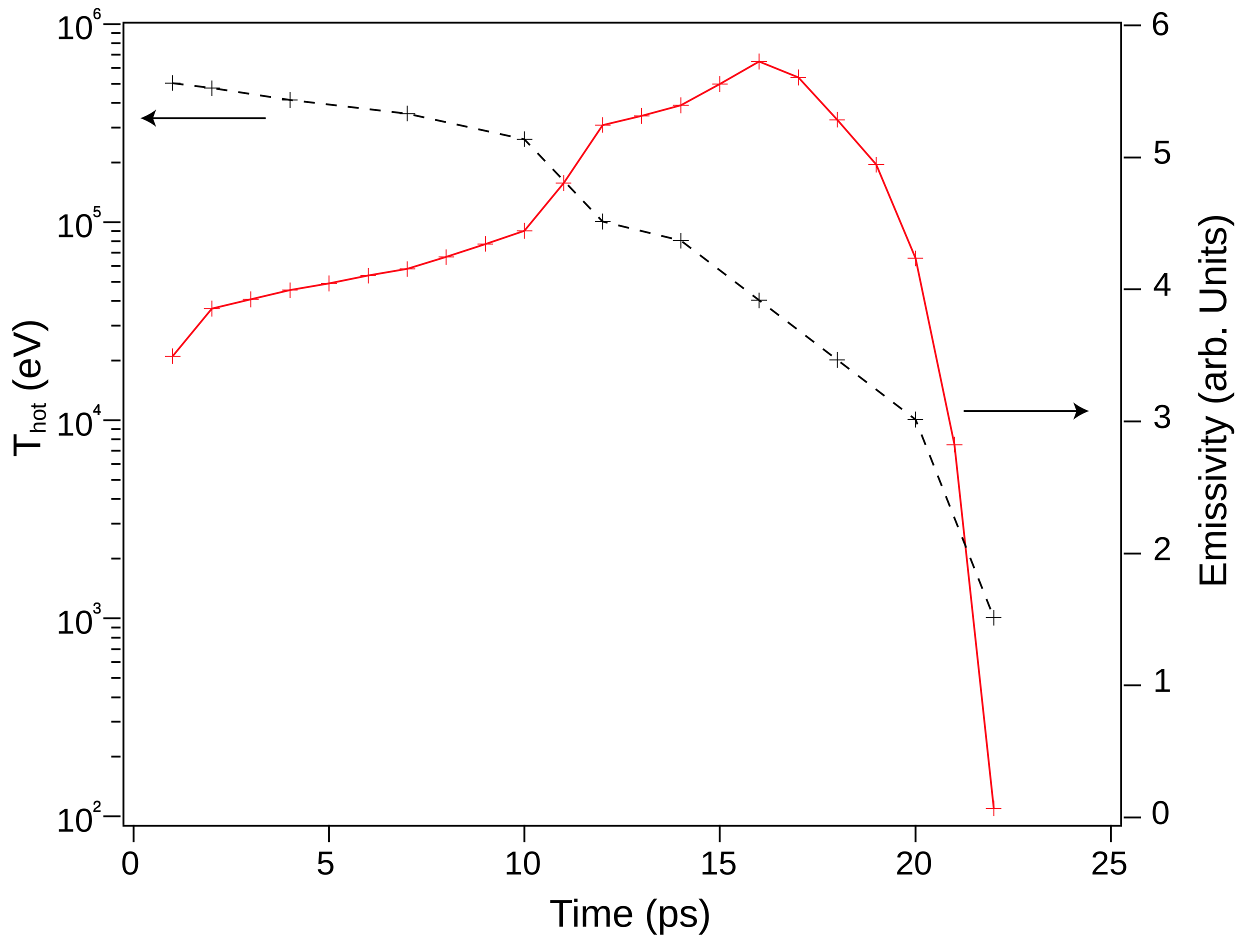

FIG. 4: Calculated total Ti K_α emissivity (solid line) as a function of time. The hot electron relaxation used in this calculation (dashed line) was predicted by the collisional model.